Characterizing the Interfiber Bonding of Paper Pulps: Tensile Behavior of Some Mathematical Models of Paper Networks.

Jack C. Smith

Polymer Science and Standards Division
National Measurement Laboratory
National Bureau of Standards

September 1, 1978

NBSIR 79-1735

CHARACTERIZING THE INTERFIBER BONDING OF PAPER PULPS: TENSILE BEHAVIOR OF SOME MATHEMATICAL MODELS OF PAPER NETWORKS.

Jack C. Smith

Polymer Science and Standards Division
National Measurement Laboratory
National Bureau of Standards

September 1, 1978

Final Report Covering the Period
April 1, 1977 through September 30, 1977

TABLE OF CONTENTS

SUMMARY AND CONCLUSIONS

The behavior of a thin web-like paper network during elongation has been approximately simulated by two simple mathematical models. One of these is a parallel-spring model consisting of a series of segments formed by connecting springs in parallel between two rigid bars. The other is a square-network model consisting of a network with square meshes formed from springs of equal length. The square-network model provides the better simulation of an actual network, but a complicated computer program is required to calculate behaviors. The parallel-spring model is mathematically simple, and can be used to suggest general behaviors which can be verified by calculations for other more suitable models.

In these studies emphasis is placed on the effect of breakage of a central bond when the model is stretched. The resulting distorted mesh configurations, the drop in tensile force, and the energy lost by the network are calculated. An attempt is made to interpret the behavior of an actual paper network in the light of these results.

There is an energy parameter E obtained experimentally by averaging the energy losses incurred in a series of bond breaks when a web-like paper network is elongated. This energy parameter has been used to characterize the adhesive force between fibers constituting the network. The model studies suggest that the values of E are approximately independent of the size and shape of the test specimens, provided the mesh sizes of the specimen networks are the same.

The model studies indicate that a force drop parameter F, analogous to the energy parameter, would be feasible for characterizing adhesion. This parameter, which has not been tested experimentally, would be obtained as the average of force drops resulting from bond breaks in a specimen as it

is elongated. According to the model studies the values of F
are approximately inversely proportional to the initial lengths
of the specimens, and approximately independent of the widths,
provided the mesh sizes of the specimen networks are the same.

The two parameters E and F are sensitive to mesh size.
The model studies suggest that if two test specimens have the
same initial lengths but different mesh sizes, the values of
E and F obtained will be approximately proportional to
lengths characterizing the mesh size of each specimen network.

Results of calculations with a square-network model show
that the energy loss incurred by any one bond break is not a
linear function of the local force at the bond. It possibly
is approximately proportional to f^α, where f is the local
force, and α is a constant between 1 and 2. For a square-
network model α is close to 1.5 .

Calculations with a square-network model show that the
force drop incurred by any one bond break is not a linear
function of the force at the bond. It possibly is proportional
to f^β, where β is a constant between 0 and 1. For a square-
network model β is close to 0.5 .

One concludes from the model studies that the parameters
E and F can characterize adhesive force between paper pulp
fibers. The parameters, however, have some objectionable
features. They are sensitive to mesh sizes and distribution
of mesh sizes in the specimen network, and they are not
linear functions of the average of the bond breaking forces.
The value obtained for one of these parameters is a complicated
function of mesh size and bond adhesive force. For instance
a formulation for the parameter E based on the square-network
model would be

$$E = \frac{1}{n} \sum_{i=1}^{n} K_i f_i^{\alpha} g(x_i)$$

where n is the number of bond breaks. K is a constant of the

network, which may change slightly from break to break. f is a local bond breaking force, and α a constant. g is a quasi-linear function of a characteristic mesh length x. A formulation for the parameter F would be similar, but different constants and functions would be used.

INTRODUCTION

In previous reports [1-3] a method has been described for characterizing the adhesion between fibers in a sheet of paper. This method consists of preparing a handsheet in the form of a low-density open web from pulp fibers to be evaluated. If a specimen from this handsheet is elongated to break in a sensitive tensile tester, a force-elongation curve containing numerous jags is obtained. Each jag is caused by the breakage of a bond between fibers constituting the handsheet network. By integrating under this curve in the vicinity of the jag it is possible to determine a characteristic energy E, related to the average stored energy that is lost per break, mostly by fibers in the vicinity of the broken bond. This energy is used as a measure of the bond adhesion between two fibers.

The selection of this parameter was an intuitive process. Its applicability must be judged on the basis of experimental evidence. What the parameter actually measures is still not well understood. Some questions that arise are: How is the strain energy distributed throughout the network after a bond break? How is the energy loss related to the local stress at the bond just before break? What is the effect of mesh size? What is the optimum specimen size and shape for tensile tests to determine the characteristic energy?

In this report two crude mathematical models of a fibrous network are described, and their behavior under elongation calculated. The concepts developed and the results obtained add to an intuitive understanding of the energy parameter.

THE PARALLEL-SPRING MODEL

The parallel-spring model is depicted schematically in figure 1. It consists of a number of springs in a series-parallel arrangement. The dots indicate where the springs are bonded to each other and to a series of rigid bars. There are 2M-1 junction points on each bar, and there are 2N-1 bars. In the unstrained state each spring has a length ℓ, called the mesh length. The spring constant is given by k/ℓ. The model is elongated so that each spring is extended an amount $\ell\delta$, where δ is the strain. The bond B then breaks, and the two springs previously joined at that point are inactivated.

The initial force sustained by the model before break is

$$F_b = (2M-1)k\delta \tag{1.1}$$

The initial elongation of the model is

$$\Delta L = 2(N-1)\ell\delta \tag{1.2}$$

The initial energy stored in the model is

$$E_b = \frac{1}{2}(2M-1)k\delta \cdot 2(N-1)\ell\delta$$

$$= 2(N-1)(2M-1)\ell \cdot \frac{1}{2}k\delta^2 \tag{1.3}$$

After the break the elongation of the model is maintained constant, and the force drops to a value F_a. The horizontal bars to which the springs are attached remain horizontal. In the two segments of the model on either side of the broken bond the force F_a is sustained by 2M-2 parallel springs, so that

$$F_a = (2M-2)k\frac{(\Delta L)_1}{\ell}$$

or

$$(\Delta L)_1 = \frac{F_a \ell}{(2M-2)k} \tag{1.4}$$

where $(\Delta L)_1$ is the elongation of the segment.

The elongation in the other $2(N-2)$ segments is given by

$$(\Delta L)_2 = \frac{F_a \ell}{(2M-1)k} \tag{1.5}$$

where $(\Delta L)_2$ is the elongation of the segment.

The total elongation of all the segments is

$$2(N-1)\ell\delta = \frac{2(N-2)F_a\ell}{(2M-1)k} + \frac{2F_a\ell}{(2M-2)k}$$

Thus

$$(2M-1)k\delta = F_b = \left\{ \frac{N-2}{N-1} + \frac{2M-1}{2(M-1)(N-1)} \right\} F_a$$

or

$$F_b = \left\{ 1 + \frac{2M-1}{2(M-1)(N-1)} - \frac{1}{N-1} \right\} F_a$$

$$= \left\{ 1 + \frac{1}{2(M-1)(N-1)} \right\} F_a$$

Hence

$$F_a = \overline{T}F_b \tag{1.6}$$

where

$$\overline{T} = \frac{2(M-1)(N-1)}{2(M-1)(N-1) + 1} \tag{1.7}$$

$\overline{T}$ is the fraction of the force remaining after a bond break. The force drop resulting from the break is given by

$$\Delta F = F_b(1-\overline{T}) \tag{1.8}$$

The energy in the two segments of the model adjoining the broken bond is

$$\frac{1}{2}(\Delta L)_1 \cdot F_a = \frac{1}{2} \frac{F_a^2 \ell}{(2M-2)k}$$

and the energy in the other $2(N-2)$ segments is

$$\frac{1}{2}(\Delta L)_2 \cdot F_a = \frac{1}{2} \frac{F_a^2 \ell}{(2M-1)k}$$

Thus the total energy is

$$E_a = 2(N-2)\cdot \frac{1}{2}\frac{\bar{F}_a^2 \ell}{(2M-1)k} + 2\cdot\frac{1}{2}\frac{\bar{F}_a^2 \ell}{(2M-2)k}$$

$$= 2\left\{\frac{N-2}{2M-1} + \frac{1}{2M-2}\right\}\cdot\frac{1}{2}\frac{\bar{F}_a^2 \ell}{k}$$

$$= \frac{2(N-1)}{2M-1}\left\{\frac{N-2}{N-1} + \frac{2M-1}{2(M-1)(N-1)}\right\}\frac{\ell}{2k}\cdot\bar{T}^2\cdot(2M-1)^2 k^2 \delta^2$$

$$= 2(N-1)(2M-1)\ell\cdot\frac{1}{\bar{T}}\cdot\bar{T}^2\cdot\frac{1}{2}k\delta^2$$

or

$$E_a = 2(N-1)(2M-1)\ell\bar{T}\,\frac{1}{2}k\delta^2$$

$$= \bar{T}E_b \qquad\qquad\qquad (1.9)$$

In order to describe the way strain energy is distrib-
uted in a model it is useful to associate energy with each
of the junction points in such a way that the sum of the
associated energies is equal to the total energy stored.
At any given junction point the associated energy is equal
to one-half the sum of the energies in the springs joined
at that point. The factor of one-half is introduced because
when the associated energies are summed over all the junction
points, the energy of each spring is counted twice. At
junction points on the top and bottom boundaries there is
only one spring, but the factor of one-half is still
necessary.

A dimensionless average associated energy $\bar{E}$ can be
defined by means of the relation,

$$E_a = (2M-1)(2N-1)\bar{E}\cdot\frac{1}{2}k\delta^2\ell \qquad\qquad (1.10)$$

The factor $(2M-1)(2N-1)$ gives the total number of points
in the network. The factor $\frac{1}{2}k\delta^2\ell$ is the energy stored in

one spring before a bond break, and is introduced into the expression to make $\overline{E}$ dimensionless. By equating relations (1.9) and (1.10) an alternative relation,

$$\overline{E} = \frac{2N-2}{2N-1} \overline{T} \tag{1.11}$$

is obtained.

The energy loss resulting from a bond break is, from eq (1.9),

$$\Delta E = E_b - E_a = (1-\overline{T})E_b \tag{1.12}$$

An alternative form is obtained from eqs (1.3) and (1.10).

$$\Delta E = 2(N-1)(2M-1)\ell(1 - \frac{2N-1}{2N-2}\overline{E}) \cdot \frac{1}{2}k\delta^2 \tag{1.13}$$

THE SQUARE-NETWORK MODEL

The square-network model is depicted schematically in figure 2. It consists of springs forming a square network. There are 2M-1 columns of junction points and 2N-1 rows of junction points. The depicted network has 7 columns (M=4) and 7 rows (N=4). The unstrained length of each spring is ℓ, and the spring constant is given by k/ℓ. The model is elongated by an amount $2(N-1)\ell\delta$. The bond at point B then breaks, and the four springs previously joined at that point are inactivated. The resulting configuration is calculated by a computer program described below.

In order to discuss the model it is convenient to identify junction points by the coordinates $i = 0, 1, \ldots m; \; j = 0, 1, \ldots n$. The corresponding numbers $I = 1, 2, \ldots M; \; J = 1, 2, \ldots N$, however, are retained for use in the formulas for force and energy, as they are more convenient for counting purposes. Because of symmetry it is only necessary to calculate the configuration of the upper right-hand quadrant; i.e., the junction points corresponding to positive values of i and j.

When the model is strained each of the junction points moves from its original position by an amount $\xi_{ij}\ell$ in the horizontal direction and $\eta_{ij}\ell$ in the vertical direction. Thus when the model is first extended and no bond break has occurred,

$$\begin{aligned} \xi_{ij} &= 0. \\ \eta_{ij} &= j\delta \end{aligned} \tag{2.1}$$

After the bond break the values of ξ_{ij}, η_{ij} readjust except for certain constraints at the boundary and the $i = 0, \; j = 0$ axes of symmetry. These are

$$\begin{aligned} \xi_{in} &= 0. \\ \eta_{in} &= n\delta \end{aligned} \tag{2.2}$$

$$\eta_{i0} = 0. \tag{2.3}$$

$$\begin{aligned} \xi_{i,-1} &= \xi_{i1} \\ \eta_{i,-1} &= \eta_{i1} \end{aligned} \tag{2.4}$$

$$\xi_{0j} = 0. \tag{2.5}$$

$$\left.\begin{array}{l} \xi_{-1j} = -\xi_{1j} \\ \eta_{-1j} = \eta_{1j} \end{array}\right\} \tag{2.6}$$

The values of ξ, η attained after bond break are found by solving a system of equations in which the horizontal and vertical forces at each junction point are balanced out, plus the boundary conditions (2.2 - 2.6). To formulate the equations applicable at the point i,j , let

$$\left.\begin{array}{l} R_A = \sqrt{(1+\Delta_A\xi)^2 + \Delta_A\eta^2} \\[10pt] R_B = \sqrt{\Delta_B\xi^2 + (1+\Delta_B\eta)^2} \\[10pt] R_C = \sqrt{\Delta_C\xi^2 + (1+\Delta_C\eta)^2} \\[10pt] R_D = \sqrt{(1+\Delta_D\xi)^2 + \Delta_D\eta^2} \end{array}\right\} \tag{2.7}$$

where Δ_A is a difference operator involving the indices $(i, i-1)$, Δ_B the indices $(j, j-1)$, Δ_C the indices $(j+1, j)$ and Δ_D the indices $(i+1, i)$. Thus, for instance, $\Delta_A\xi$ means $\xi_{ij} - \xi_{i-1,j}$. The quantities $R\ell$ are the distances from a point ij to an adjacent point. The horizontal force balance equation is then

$$\frac{k(R_D-1)(1+\Delta_D\xi)}{R_D} + \frac{k(R_C-1)\Delta_C\xi}{R_C}$$
$$= \frac{k(R_B-1)\Delta_B\xi}{R_B} + \frac{k(R_A-1)(1+\Delta_A\xi)}{R_A}$$

or

$$(1+\Delta_D\xi)(1-1/R_D) + \Delta_C\xi(1-1/R_C)$$
$$- \Delta_B\xi(1-1/R_B) - (1+\Delta_D\xi)(1-1/R_D) = 0. \tag{2.8}$$

Similarly for the vertical components

$$\Delta_D\eta(1-1/R_D) + (1+\Delta_C\eta)(1-1/R_C)$$
$$- (1+\Delta_B\eta)(1-1/R_B) - \Delta_A\eta(1-1/R_A) = 0. \tag{2.9}$$

Equations (2.8) and (2.9) apply at the general junction point ij, but when i = 0, m or j = 0, n they must be modified to conform with boundary or symmetry conditions.

It should be noted that the horizontal forces acting at a point i,j are dependent mostly upon the values of $\xi_{i-1,j}$, ξ_{ij} and $\xi_{i+1,j}$. Therefore eq (2.8) which has the form

$$f(\xi_{i-1,j}, \eta_{i-1,j}, \xi_{ij}, \eta_{ij}, \xi_{i+1,j}, \eta_{i+1,j},$$
$$\xi_{i,j-1}, \eta_{i,j-1}, \xi_{i,j+1}, \eta_{i,j+1}) = 0. \tag{2.10}$$

was expressed as a Taylor's series expansion in terms of only these three most important variables to become

$$f^{(k)} + \left(\frac{\partial f}{\partial \xi_{i-1,j}}\right)^{(k)} \Delta \xi_{i-1,j} + \left(\frac{\partial f}{\partial \xi_{ij}}\right)^{(k)} \Delta \xi_{ij}$$

$$+ \left(\frac{\partial f}{\partial \xi_{i+1,j}}\right)^{(k)} \Delta \xi_{i+1,j} = 0. \tag{2.11}$$

where the $\Delta \xi_{ij}$ means $\xi_{ij}^{(k+1)} - \xi_{ij}^{(k)}$ and $\Delta \xi_{i-1,j}$ and $\Delta \xi_{i+1,j}$ have similar meanings. $f^{(k)}$, $\left(\frac{\partial f}{\partial \xi_{ij}}\right)^{(k)}$ etc. are evaluated as functions of $\xi^{(k)}$, $\eta^{(k)}$. The values of $\xi^{(k+1)}$ are obtained by solving the system of equations (2.11) corresponding to different values of j.

A set of five of these equations, for instance, would look like

$$B_1 x_1 + C_1 x_2 \qquad\qquad\qquad = K_1$$
$$A_2 x_1 + B_2 x_2 + C_2 x_3 \qquad\qquad = K_2$$
$$A_3 x_2 + B_3 x_3 + C_3 x_4 \qquad = K_3$$
$$A_4 x_3 + B_4 x_4 + C_4 x_5 = K_4$$
$$A_5 x_5 + B_5 x_5 = K_5$$

This set of equations is easily solved by a Gauss-Jordan reduction.

Equations (2.11) are solved to obtain values of $\xi^{(k+1)}$.
Similarly eq (2.9) can be expanded in terms of $\eta_{i,j-1}, \eta_{ij}$
and $\eta_{i,j+1}$. The set of equations obtained for different
values of i can be solved to obtain values of $\eta^{(k+1)}$. The
values of $f, \left(\dfrac{\partial f}{\partial \xi_{ij}}\right), \left(\dfrac{\partial f}{\partial \eta_{ij}}\right)$ in eq (2.11) for ξ and the corre-
sponding equation for η are then evaluated using $\xi^{(k+1)}, \eta^{(k+1)}$
and the procedure iterated to obtain $\xi^{(k+2)}, \eta^{(k+2)}$.

During the calculation process solutions for ξ and η
may be obtained such that R_A, R_B, R_C, or R_D becomes less than
1 in value. This means that there is a spring in compression.
This situation is not permitted as it is more realistic to
assume that the spring would buckle rather than resist a
compressive force. Therefore if there is an R less than 1 ,
modified equations in which the influence of the spring is
removed are used in an alternate calculation.

The configuration of the network can be calculated in
other ways. For instance eqs (2.8) and (2.9) could be
expanded in the variables ξ_{ij}, η_{ij}. Improved approximations
for ξ, η could be obtained by solving only two simultaneous
equations at each point, but a very large number of iterations
would be required to obtain very precise values of ξ, η. On
the other hand the equations could be expanded in terms of
all 10 variables. In this way a system of approximately MN
equations in MN unknowns would be obtained. If these equations
had a numerically stable solution and round-off errors were
not too severe, only a few iterations might be required.

The method of solution that was used was a compromise
between these two extremes. It appears to be stable but in
most cases requires 100 or 200 iterations to obtain satis-
factorily precise values. When situations are calculated in
which the initial strain δ is of the order of one percent,
more than 200 iterations may be required. In this situation
the values of some Rs are very close to unity and very small
values of R-1 are obtained. Thus it might be better in this

case to rewrite eqs (2.8) and (2.9), expressing terms of the form (1-1/R) as a truncated series, although this was not done for the calculations reported here.

After sufficiently accurate values of ξ and η were obtained, the tensile force T_{in} at the top of each column of springs was calculated using the formula

$$\left.\begin{aligned} T_{in} &= k(1+n\delta-\eta_{i,n-1})(1-1/R_B) \\ R_B &= \sqrt{\xi_{i,n-1}^2+(1+n\delta-\eta_{i,n-1})^2} \end{aligned}\right\}$$ (2.12)

When i = 0, the value of T_{0n} simplifies to

$$T_{0n} = k(n\delta-\eta_{0,n-1})$$ (2.13)

The force after break F_a then becomes

$$F_a = T_{0n} + 2\sum_{i=1}^{n}T_{in}$$ (2.14)

The fraction of the force remaining after a bond break $\bar{T}$ is given by the ratio F_a/F_b.

The average associated energy $\bar{E}$ is found from its definition, eq (1.10), after calculating the associated energy for each junction point and summing over all the junction points to obtain the stored energy after break E_a.

The value of $\bar{E}$ can be obtained by a different calculation, if F_a is known as a function of δ from a series of calculations on a given model. The energy after break E_a is found by integrating under the curve of F_a versus initial elongation $\Delta L = 2(N-1)\ell\delta$. Thus,

$$E_a = \int_0^{2(N-1)\ell\delta} F_a \cdot d[2(N-1)\ell\delta]$$

$$= 2(N-1)(2M-1)k\ell\int_0^{\delta}\bar{T}\delta d\delta$$ (2.15)

From the definition eq (1.10) $\overline{E}$ is then given by

$$\overline{E} = \frac{2N-2}{2N-1} \cdot \frac{2}{\delta^2} \int_0^\delta \overline{T}\delta\,d\delta \tag{2.16}$$

In the square-network model $\overline{T}$ is not a constant independent of δ as it is in the parallel-spring model. If $\overline{T}$ were constant, eq (2.16) would reduce to the relation eq (1.11) given for the parallel-spring model.

It should be noted that the behavior of the square-network model is the same as that of the parallel-spring model before the central bond breaks. Therefore eqs (1.1), (1.2) and (1.3) are the same for both models. The quantity $\overline{T}$ is defined by eq (1.6) and the quantity $\overline{E}$ by eq (1.10) in both models. Therefore eqs (1.8) and (1.13) are valid for both models. Relation (2.16) is a general definition valid for both models, but relations (1.7) and (1.11) apply to the parallel-spring model only. Therefore eqs (1.9) and (1.12) also are valid only for the parallel-spring model.

SQUARE-NETWORK MODEL CALCULATIONS

A number of calculations were carried out for different square-network models to determine the number of iterations required for accurate values of $\overline{T}$ and $\overline{E}$. The model for which M=11, N=21, ℓ=1 was studied the most extensively. Results of calculations for this model are given in table 1. These results indicate that for values of δ greater than 0.05, 100 or 200 iterations are required to obtain values of $\overline{T}$ and $\overline{E}$ accurate to more than four significant digits. When δ is 0.05 or less, more than 200 iterations are desirable. Check calculations were also carried out on the other models studied, and 200 iterations were determined as sufficient.

Calculations were carried out on five different models. The initial strain δ for these models was 0.20 . A mesh length of ℓ=1 was assumed for the calculations. Values of M and N were varied in order to study how $\overline{T}$ and $\overline{E}$ depended on the shape and on the number of junctions in the model. Results of the calculations for these models are given in table 2.

The configuration of the model for which M=11, N=21 is plotted in figure 3. Only the upper right-hand quadrant of the model is shown, as the complete model is symmetrical with respect to this quadrant. The distortion due to the bond break is seen to be concentrated along the central column of springs (I=1). Buckling occurs (R<1) in the regions where the springs are indicated by dotted lines. Although not easily discernable in the figure, the central width (J=1) has been reduced to 0.956 times the original width, as a result of bond break.

An energy map of the model for which M=11, N=21 is shown as an isometric plot in figure 4. As before only the upper right-hand quadrant of the model is shown. The dimensionless value plotted at each junction point is the ratio of the associated energy after bond break to the associated energy before bond break. According to this map the associated energy remains constant at most of the junction points, it increases at points immediately to the right and left of the broken bond

and decreases to a lower level at junction points above and below the broken bond.

Figure 5 shows the configuration after bond break, and figure 6 shows the energy map of the model for which M=21, N=41 . This model, of the same shape as the previous model, has approximately four times as many junction points. The corresponding figures for the two models are similar.

Table 3 presents values of $\overline{T}$ and $\overline{E}$ as functions of initial strain δ in the case of the model for which M=11, N=21. A force-elongation curve for this model after one central bond has been broken can be plotted using data from table 3. The force has the value $(2M-1)\overline{T}k\delta$, and elongation the value $2(N-1)\ell\delta$. The essential characteristics of the curve are shown by figure 7, which is a plot of $\overline{T}\delta$ vs δ for this model. Unfortunately the values of $\overline{T}$ are so close to unity that this curve lies very close to the force-elongation curve, shown as a dashed line, of the model before the central bond was broken, and the non-linear character of the curve is not readily apparent.

The non-linear character of the force-elongation curve can be demonstrated by plotting the difference in force before and after break as a function of δ. This is shown in figure 8, in which $(1-\overline{T})\delta$ is plotted vs δ . As a matter of interest $(1-\overline{T})$ for the parallel-spring model (M=11, N=21) was calculated. Its value was 0.0024938 . The linear function 0.0024938δ is shown as a dashed line on the plot. The value of $\overline{T}$ for the parallel-spring model exceeds the values of $\overline{T}$ calculated for the square-network model. Evidently the force drop incurred by a bond break in the square-network model is greater than the force drop incurred in the parallel-spring model.

The area under the $\overline{T}\delta$ curve in figure 7 is equal to $\int_{0}^{\delta}\overline{T}\delta d\delta$, and according to eq (2.16) the average associated $\overline{E}$ is equal to $\dfrac{2N-2}{2N-1}\cdot\dfrac{2}{\delta^{2}}$ times this quantity. Thus values of

$\bar{E}$ can be calculated from $\bar{T}$ and δ according to eq (2.16) and the result compared with the values of $\bar{E}$ in table 3, which were calculated from the associated energies present after break. This should provide a check on the accuracy of the computer calculations. The results of this calculation are given in the last column of table 3. The values of $\bar{E}$ obtained by the two methods are seen to be in fair agreement.

DISCUSSION OF RESULTS

1. Configurational Distortions and the Redistribution of
   Associated Energies as the Result of a Bond Break.

It has been assumed that in a low-density paper network of the type tested experimentally [1-3], in most cases a bond break results only in local distortions, and most of the energy loss is also concentrated locally. It would be desirable to demonstrate this with a mathematical model, but the square-network model is not suitable for this purpose. The distortions and energy losses are concentrated along the column of springs directly in line with the broken bond. Possibly a better model would be one in which the meshes were of a different shape, such as a hexagon, and so arranged that load bearing fibers could not be easily aligned in the direction of stretch. Such a model would require less stretching force, have a nonlinear force-elongation curve, and probably have a greater tendency to buckle laterally. It would better simulate the behavior of a thin paper network, but at the price of greater mathematical complexity.

In the energy maps, figures 4 and 5, there is an increase in associated energy at the junctions to either side of the broken bond. These bonds therefore should break immediately after breakage of the central bond, and bonds farther out should break successively in a tearing action that proceeds across the model network. This tearing action is probably common to many models, and actually occurs in real paper networks. In the paper networks however it seldom goes to completion, because the density of fibers is not sufficiently uniform.

2. The Effect of Mesh Length

In experimental work specimens of standard dimensions (usually 2x1 cm) are elongated, and the applied force recorded as a function of the elongation. Whenever a bond breaks the

force decreases sharply, and the energy loss resulting from the bond break can be determined by integrating under the force-elongation curve in the vicinity of the force drop. Certain of these energy losses are averaged to obtain a parameter characterizing bond strength.

If it is assumed that all of the breaks occur at approximately the same local force level, and the specimens have uniform mesh size, this energy parameter might provide a reliable indication of the relative bond strength. For instance bonding could be studied in thin handsheets of the same mass per unit area made from a pulp that had been subjected to various beating treatments. However if one attempts to compare bonding in standard handsheets made from different pulps, a difficulty arises. One pulp may be coarser than the other. Thus a handsheet of a standard mass per unit area made from a coarse pulp would have fewer bonded junctions and larger meshes on the average than would a handsheet made from a finer pulp. In order to compare energy parameters for these different pulps it is necessary to know what is the effect of mesh size.

To study this effect in models, consider two parallel-spring models: model A; $M=11$, $N=21$, $\ell=1$ and model B; $M=21$, $N=41$, $\ell=0.5$. These models have the same external dimensions, but the mesh length of model B is half that of model A. Let the two models be extended the same amount, so that δ and therefore the local force $k\delta$ is the same in each. From eqs (1.1), (1.7) and (1.8) the force drop in model A is $21k\delta/401 \sim 0.05k\delta$, and in model B is $41k\delta/1601 \sim 0.026k\delta$. From eqs (1.3), (1.7) and (1.12) the energy loss in model A is $\frac{840}{401}\cdot\frac{1}{2}k\delta^2 \sim 2.1\cdot\frac{1}{2}k\delta^2$, and in model B is $\frac{1640}{1601}\cdot\frac{1}{2}k\delta^2 \sim 1.02\cdot\frac{1}{2}k\delta^2$. Evidently model B with half the mesh size of model A also has approximately half the force drop and half the energy loss.

In any parallel-spring model, from eqs (1.1), (1.7) and (1.8)

$$\Delta F = \frac{(2M-1)k\delta}{2(M-1)(N-1) + 1} = \frac{2(M-1) + 1}{2(M-1)(N-1) + 1}k\delta$$

which for large M becomes

$$\Delta F \sim \frac{1}{N-1}k\delta$$

Substituting the initial length $L=2(N-1)\ell$ into this expression gives

$$\Delta F \sim \frac{2\ell}{L} k\delta \qquad\qquad (4.1)$$

From eqs (1.3), (1.7) and (1.12)

$$\Delta E = \frac{2(N-1)(2M-1)\ell}{2(M-1)(N-1) + 1} \cdot \frac{1}{2}k\delta^2$$

$$= \frac{2(N-1)(2M-2) + 2(N-1)}{2(M-1)(N-1) + 1}\ell \cdot \frac{1}{2}k\delta^2$$

which for large M becomes

$$\Delta E \sim 2\ell \cdot \frac{1}{2}k\delta^2 \qquad\qquad (4.2)$$

According to eqs (4.1) and (4.2), if any two parallel-spring models for which M is large are extended so that the local force $k\delta$ is the same in each model, the ratio of the energy losses $\Delta E_1/\Delta E_2$ in the two models will be the same as the ratios of the respective mesh lengths ℓ_1/ℓ_2. If in addition the initial lengths of the two models are the same; i.e., $2(N_1-1)\ell_1=2(N_2-1)\ell_2$, the ratios of the force drops will be equal to ℓ_1/ℓ_2.

Table 4 gives the results of calculations for a number of parallel-spring models, all of which have the same initial length. According to these results the force drops and energy losses are almost linearly proportional to the mesh length ℓ, despite the relatively low value of M in some of these models. It is interesting to observe that values of total force before break F_b and the total energy before break E_b do not influence these results significantly. The values of F_b and E_b are proportional to 2M-1 however, so this is just a manifestation

of the near independence of the values of ΔF and ΔE on the
values of M, for M sufficiently large (e.g., M=11).

Table 5 gives results of calculations for some square-
network models having the same initial length. The M, N and
ℓ parameters for these models are the same as those in table 4.
The force drops and energy losses for these models decrease
as the mesh length ℓ decreases, but are not linearly propor-
tional to the mesh length. For instance the three models for
which M=11 have ℓ ratios of 1.0:0.50:0.25, ΔF ratios of
1.0:0.57:0.31 and ΔE ratios of 1.0:0.64:0.37. The two models
for which M=21 have ℓ ratios of 1.0:0.50, ΔF ratios of
1.0:0.54 and ΔE ratios of 1.0:0.58. Apparently the dependence
of ΔF and ΔE upon ℓ becomes more linear as M increases.

Results for the parallel-spring and square-network models
suggest that the force drops and energy losses observed in
a paper fiber network have an approximately linear dependence
on a characteristic mesh length. The actual dependence,
however, must be determined experimentally.

The effect of mesh length can also be deduced by a
different argument as follows: Select a model (M,N) for which
calculations have been made so that $\overline{T}$ and $\overline{E}$ are known for a
given δ ; i.e., $\overline{T}=\overline{T}(\delta)$, $\overline{E}=\overline{E}(\delta)$. Select a mesh length ℓ . The
initial length of the model then is $2(N-1)\ell$. For each mesh
length selected the model is elongated an amount $\Delta I=2(N-1)\ell\delta$.
This assures that the local tension at the bond break is
always the same $(k\delta)$. From eqs (1.1), (1.8) and (1.13)

$$\Delta F = (2M-1)(1-\overline{T})k\delta \tag{4.3}$$

$$\Delta E = 2(N-1)(2M-1)\ell(1-\frac{2N-1}{2N-2}\overline{E})\cdot\frac{1}{2}k\delta^2 \tag{4.4}$$

As $\overline{T}$ and $\overline{E}$ are functions of δ which is kept constant, ΔF
is a constant independent of mesh length and ΔE is directly
proportional to the mesh length. This conclusion is valid
for either the parallel-spring or square-network type of model.

The conclusion just obtained seems to conflict with that
found by the analysis presented above. However in that analysis

a number of models of different mesh length but having the
same initial length were elongated, whereas in the present
analysis the initial length of the model depends on the mesh
length.

This latter deduction may be useful in experimental work,
as illustrated in the following situation: Suppose that two
handsheets have been manufactured from the same pulp stock.
Let the first handsheet have twice the areal density as the
second, so that its characteristic mesh length is one-half
as large. According to the analysis above, bond breaks in both
handsheets should occur at the same force level, but a specimen
from the second handsheet must be extended twice as much as
one from the first in order to attain this force. Thus the
average energy loss per bond break in the second handsheet
should be twice that in the first. This suggests that energy
parameters found by tests on handsheets of different areal
density can be scaled to find the value corresponding to a
standard mesh length.

3. The Effect of Sample Size and Shape

If several models, each with the same mesh length λ, are
elongated to the same tension, the force drops and energy
losses are given by eqs (4.3) and (4.4). For square-network
models it is necessary to know the appropriate values of $\overline{T}$
and $\overline{E}$ before the effects of sample size can be predicted.
For parallel-spring models however, simple expressions for
$\overline{T}$ and $\overline{E}$ are known, so that for large values of M eqs (4.1)
and (4.2) apply. Equation (4.1) predicts that the product of
the force drop by the length of the specimen, $L\Delta F$, is a
constant for all models having the same mesh length λ, and
eq (4.2) then states that the energy losses are constant.

Table 6 gives values of the force drop and energy loss
for some parallel-spring models. Note that the quantities
$L\Delta F/k\delta\lambda$ and $\Delta E/0.5k\delta^2\lambda$ have the same value in this table

because of the choice of units. It is apparent that ΔF and
ΔE for parallel-spring models are closely predicted by
eqs (4.1) and (4.2). The three models for which M=11
(and width $W=2(M-1)\ell=20\ell$) have values for $L\Delta F$ and ΔE of
approximately 2.095, and the two models for which M=21 ($W=40\ell$)
have values of approximately 2.048. Evidently $L\Delta F$ and ΔE
approach a value of 2.0 with increasing M, as they should
according to eqs (4.1) and (4.2).

Table 7 gives values of the force drop and energy loss
for some square-network models. The values of $L\Delta F$ and ΔE for
these models are roughly constant, but there seems to be
some dependence upon both M and N. For instance the three
models for which M=11 ($W=20\ell$) have lengths that increase in
the ratio 20:40:80. The $L\Delta F$ values for these models are
10.27:11.79:12.80 . The two models for which M=21 ($W=40\ell$)
have length ratios of 40:80 and $L\Delta F$ values of 11.30:12.27 .
Similar results are obtained for the ΔE values.

The results for the square-network models suggest that
various values of $L\Delta F$ and ΔE obtained by tests on specimens of
the same characteristic mesh length but of different size and
shape, are roughly comparable. For most accurate results
however all test specimens should have the same standardized
dimensions.

For the parallel-spring models, from eqs (1.1), (1.3),
(1.8) and (1.12)

$$\frac{\Delta E}{\Delta F} = \frac{E_b}{F_b} = \frac{2(N-1)\ell\delta}{2} = \frac{L\delta}{2} \tag{4.5}$$

This equation states that for the parallel-spring models the
ratio $\Delta E/\Delta F$ is proportional to the average elongation at
which bond breaks occur, regardless of the value of M.
Experimentally it is desirable to have significantly large
force drops for a given energy loss, so the ratio $\Delta E/\Delta F$
should be kept small by making L as small as feasible.

For the square-network models, from eqs (4.3) and (4.4)

$$\frac{\Delta E}{\Delta F} = [(1 - \frac{2N-1}{2N-2}\overline{E})/(1-\overline{T})] \frac{L\delta}{2} \tag{4.6}$$

Table 8 gives values for the ratio $\Delta E/\Delta F$ for some square-network models. Parallel-spring models have values of $\Delta E/\Delta F$ that are proportional to the initial length L in accordance with eq (4.5), but for the square-network models the dependence of $\Delta E/\Delta F$ upon L is not quite linear, and there also seems to be a small dependence upon M. This is best shown by comparing values of the quantity $\frac{2}{L\delta}\left(\frac{\Delta E}{\Delta F}\right)$, which for parallel-spring models is equal to unity but for the square-network models in table 8 varies between 1.2 and 1.5 depending upon the model.

Of most importance, however, is the confirmation that the quantity $\Delta E/\Delta F$ can be kept low by choosing a small value of L. This situation is limited somewhat in experimental tests. A specimen length at least twice the specimen width is preferred, in order to avoid excessive stress distortion near the clamps.

Although the results of tables 7 and 8 indicate that the values of $L\Delta F$, ΔE and $\Delta E/L\Delta F$ are insensitive to the value of M, there are circumstances where it is advantageous to vary the width of the specimen, as in the following experimental situation: Suppose that tests are being conducted on a given specimen, but the force drops observed are small, so that they cannot be measured with much certainty. The calculation of energy loss requires that the force drop be known as accurately as possible. Thus the experimental length should be small in order that the force drop be large. Further improvement is then achieved by decreasing the specimen width. This decreases the value of force at break F_b without significantly affecting the value of the force drop. The amplification of the recording instrument can then be increased and the force drop better resolved.

4. Dependence of Energy Loss Upon the Local Breaking Force.

According to eq (4.4) the energy loss ΔE is proportional to the product of the quantity $(1 - \frac{2N-1}{2N-2}\bar{E})$ by the square of the local breaking force $k\delta$. For parallel-spring models $\bar{E}$ and therefore the quantity $(1 - \frac{2N-1}{2N-2}\bar{E})$ is independent of the value of this force. Thus for these models energy loss is proportional to the square of the local force at break. For square-network models however the value of $\bar{E}$ depends upon the value of δ, so this simple quadratic relationship no longer applies.

Figure 9 is a plot of the quantity $(1 - \frac{2N-1}{2N-2}\bar{E})\delta^2$ as a function of δ. The ordinate in this case is proportional to the energy loss in a square-network model for which M=11 and N=21. This relationship, calculated from the data of table 3, is shown by the solid line. A relationship having the same value for $\delta=0.10$, but for which the ordinate is of the form $K\delta^2$, where K is a constant, is shown by the dashed line. A corresponding relationship of the form $K'\delta^{1.5}$ is given by the dotted line. This latter relationship provides a better fit to the data than does the quadratic relationship.

The relationship between energy loss and local breaking force in an experimental test specimen is not known, and it does not seem feasible to determine it experimentally. It is possible that further studies with other more realistic mathematical models may provide more information on this relationship.

5. Interpretation of the Energy Parameter.

In the introduction an energy parameter E for characterizing the adhesion between pulp fibers was described. This energy parameter is obtained experimentally by elongating thin web-like specimens in a sensitive tensile tester, and measuring the energy loss incurred each time a bond breaks, as denoted by a sharp drop in the force-elongation curve. The energy losses for a selected number of bond breaks are then averaged.

The parameter E is supposed to provide a measure of the adhesive force between fibers, but the previous discussion shows that E depends on the structure of the specimen network as well. The meshes in a specimen network range over a variety of sizes, and the energy loss incurred by a break depends upon the size of the hole that opens up. If all the bonds in the neighborhood were of the same strength the parameter E would roughly measure that strength, but could still take on a range of values depending on the size distribution of the meshes in the specimen network.

The force of adhesion between fibers in the network varies from bond to bond. It has just been shown that the energy loss incurred as the result of a bond break is not linearly related to the local breaking force at the bond. Therefore the average of a number of energy losses does not reflect a simple average of the local breaking forces.

Results of calculations with square-network models suggest that the energy loss has only an approximate linear relationship to the mesh length. This introduces a slight additional complication in the interpretation of what the E parameter actually measures.

The interpretation of the E parameter may perhaps be better expressed by the following formulation: Let the energy losses be measured for each of a series of n breaks, and let the energy loss ΔE_i for the ith break be given by

$$\Delta E_i = K_i f_i^{\alpha} g(x_i)$$

K_i is a constant of the network that may vary from break to break if the network is significantly altered by the breaks. f_i is the local force on the bond at break, and α is a constant having a value probably between 1 and 2. For a square-network model α has a value close to 1.5 . $g(x_i)$ represents the functional dependence of ΔE_i upon a characteristic mesh length x_i associated with the bond i. This

relationship is probably almost a linear one.

Under these assumptions the characteristic energy E is given by

$$E = \frac{1}{n}\sum_{i=1}^{i=n} x_i f_i^{\alpha} g(x_i) \tag{4.7}$$

This formula gives an approximate idea of the nature of the parameter E. However one should remember that this formula is based on the results of square-network model calculations, and that the square-network model is only a crude representation of the paper networks that are tested experimentally. It is likely that work with more appropriate models will provide an improved understanding of the nature of E.

6. An Alternative Force Drop Parameter.

Adhesion between pulp fibers could be characterized alternatively by means of a force drop parameter F. This parameter could be obtained by averaging force drops incurred in a series of bond breaks when a test specimen is elongated. The parameter F has not been tested experimentally, but its use as a parameter to characterize adhesion seems feasible.

In order to calculate an energy parameter E it is necessary to know the slope of the force-elongation curve in the vicinity of a force drop. The force drop parameter F could be calculated more simply, as only the force drops are used.

In order that the force drop parameters be comparable, the test specimens must all have the same initial length. In other respects the force drop parameter F is similar to the energy parameter E. Both parameters are sensitive to mesh size and mesh size distribution in the test specimen network. Neither parameter is linearly related to the average of the local bond breaking force. However the functional dependence of F upon the average bond breaking force is different from that of E.

According to eq (4.3) the local force drop resulting from

a bond break is proportional to the quantity $(1-\bar{T})\delta$. A plot of $(1-\bar{T})\delta$ vs δ, which is proportional to the bond breaking force, is depicted in figure 8 for a square-network model with M=11, N=21. This curve can be fitted approximately by the curve $(1-\bar{T})\delta \sim 0.0068716\delta^{0.5}$. It can be inferred from this result that the parameter F might not increase as rapidly with increase of local adhesive force as would be desired. Parameter E with its possible $f^{1.5}$ dependence may be superior in this respect.

The dependence of parameter F upon local adhesive forces and upon mesh size is somewhat like that of parameter E. A suggested formula to express this dependence would be similar to eq (4.7) with different values for K and α, and a slightly different quasilinear function g.

REFERENCES

1. J. C. Smith and E. L. Graminski, Characterizing the Interfiber Bond Strengths of Paper Pulps in Terms of a Breaking Energy, Progress report covering the period Jan. 1, 1976 to June 30, 1976, NBSIR 76 - 1148. Available from National Technical Information Service, PB 264,689.

2. J. C. Smith and E. L. Graminski, Characterizing the Interfiber Bond Strength of Paper Pulps in Terms of a Breaking Energy: Effect of Beating, Progress report covering the period July 1, 1976 through Sept. 30, 1976, NBSIR 77 - 1286. Available from National Technical Information Service, PB 276,473.

3. J. C. Smith and E. L. Graminski, Characterizing the Interfiber Bonding of Paper Pulps: Effect of Preparation Pressure on Tensile Test Specimens, Progress report covering the period Oct. 1, 1976 through March 31, 1977, NBSIR 78 - 1459. Avaliable from National Technical Information Service, PB 280,279.

Table 1.

Values of $\bar{T}$ and $\bar{E}$ as Functions of Number of Iterations for a Square-Network Model
$M=11$, $N=21$, $\ell =1$

δ	No. of Iterations	$\bar{T}$	$\bar{E}$
0.01	100	0.95227	0.92923
	200	0.95254	0.92923
0.03	100	0.95779	0.93112
	200	0.95714	0.93100
0.05	20	0.96738	0.93606
	50	0.96679	0.93583
	100	0.96614	0.93567
	200	0.96564	0.93561
0.10	20	0.97806	0.94643
	50	0.97829	0.94638
	100	0.97827	0.94637
0.15	20	0.98316	0.95270
	50	0.98330	0.95263
	100	0.98332	0.95262
0.20	10	0.93787	0.97979
	20	0.98371	0.95679
	50	0.98594	0.95644
	100	0.98595	0.95641
	200	0.98597	0.95640

Table 2.

Values of $\overline{T}$ and $\overline{E}$ for Some Square-Network Models
$\delta = 0.20$, $\ell = 1$, 200 iterations

M	N	$\overline{T}$	$\overline{E}$
11	11	0.97554	0.92306
11	21	0.98597	0.95640
21	21	0.99311	0.96639
11	41	0.99238	0.97634
21	41	0.99626	0.98221

Table 3.

Values of $\overline{T}$ and $\overline{E}$ as Functions of Initial
Strain   for a Square-Network Model
M=11, N=21, l =1

δ	$\overline{T}$	$\overline{E}$	$\overline{E}$ eq (2.16)
0.01	0.95254	0.92923	0.92931
0.03	0.95714	0.93100	0.93230
0.05	0.96564	0.93561	0.93658
0.08	0.97477	0.94270	0.94328
0.10	0.97827	0.94637	0.94683
0.13	0.98173	0.95052	0.95078
0.15	0.98332	0.95262	0.95273
0.18	0.98507	0.95510	0.95503
0.20	0.98597	0.95640	0.95626

Note: $\overline{T}$ for the parallel-spring model is 0.99751
      $\overline{E}$ for the parallel-spring model is 0.97318

Note: Values for δ=0.01, 0.03, 0.05 and 0.20 were obtained
      after 200 iterations. All other values were obtained
      after 100 iterations.

Table 4.

Force Drops ΔF and Energy Losses ΔE for Some Parallel-Spring Models. [1]

M	N	ℓ	$F_b/k\delta$	$E_b/0.5k\delta^2$	$\Delta F/k\delta$	$\Delta E/0.5k\delta^2$
11	11	1.0	21.	420.	0.1045	2.090
11	21	0.5	21.	420.	0.0524	1.047
21	21	0.5	41.	820.	0.0512	1.024
11	41	0.25	21.	420.	0.0262	0.524
21	41	0.25	41.	820.	0.0256	0.512

Table 5.

Force Drops ΔF and Energy Losses ΔE for Some Square-Network Models. [1]

M	N	ℓ	$F_b/k\delta$	$E_b/0.5k\delta^2$	$\Delta F/k\delta$	$\Delta E/0.5k\delta^2$
11	11	1.0	21.	420.	0.5137	12.931
11	21	0.5	21.	420.	0.2946	8.270
21	21	0.5	41.	820.	0.2825	7.749
11	41	0.25	21.	420.	0.1600	4.811
21	41	0.25	21.	820.	0.1533	4.520

1. Initial length $L = 2(N-1)\ell = 20.$ for all models.

Table 6.

Values of Force Drop ΔF and Energy Loss ΔE
for Some Parallel-Spring Models.

M	N	L/ℓ	$\Delta F/k\delta$	L$\Delta F/k\delta\ell$	$\Delta E/0.5k\delta^2\ell$
11	11	20	0.1045	2.090	2.090
11	21	40	0.0524	2.095	2.095
21	21	40	0.0512	2.047	2.047
11	41	80	0.0262	2.097	2.097
21	41	80	0.0256	2.049	2.049

Table 7.

Values of Force Drop ΔF and Energy Loss ΔE
for Some Square-Network Models.

M	N	L/ℓ	$\Delta F/k\delta$	L$\Delta F/k\delta\ell$	$\Delta E/0.5k\delta^2\ell$
11	11	20	0.5137	10.27	12.93
11	21	40	0.2946	11.79	16.54
21	21	40	0.2825	11.30	15.50
11	41	80	0.1600	12.80	19.25
21	41	80	0.1533	12.27	18.08

Table 8.

Values of $\Delta E/\Delta F$ for Some Square-Network Models.

M	N	L/ℓ	$\dfrac{1}{\ell\delta}\dfrac{\Delta E}{\Delta F}$	$\dfrac{2}{L\delta}\dfrac{\Delta E}{\Delta F}$
11	11	20	12.59	1.259
11	21	40	28.07	1.403
21	21	40	27.43	1.372
11	41	80	60.14	1.503
21	41	80	58.96	1.474
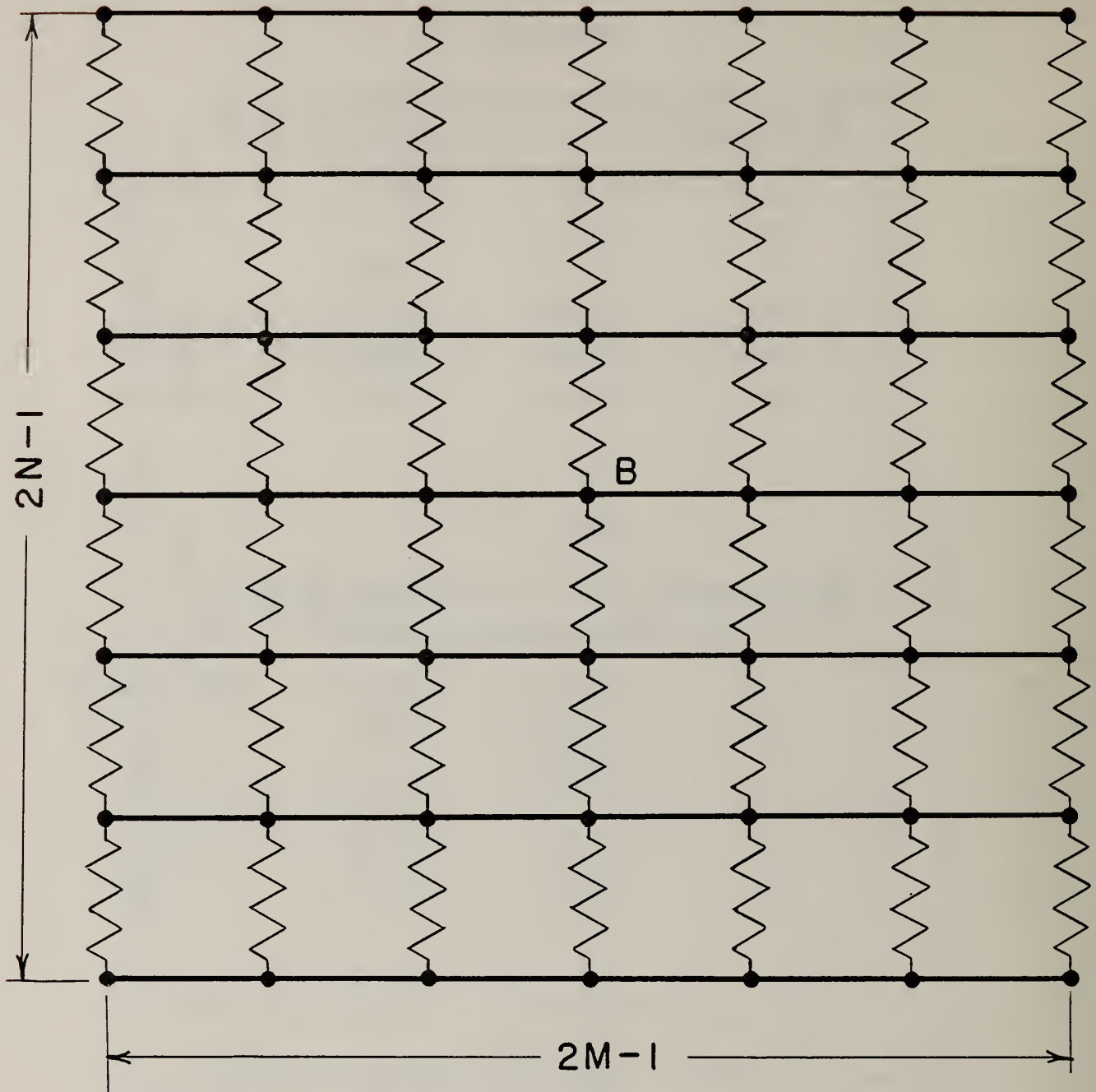
Figure 1.
Schematic representation of parallel-spring model. Model has 2M-1 parallel columns of springs attached to 2N-1 rigid transverse bars.
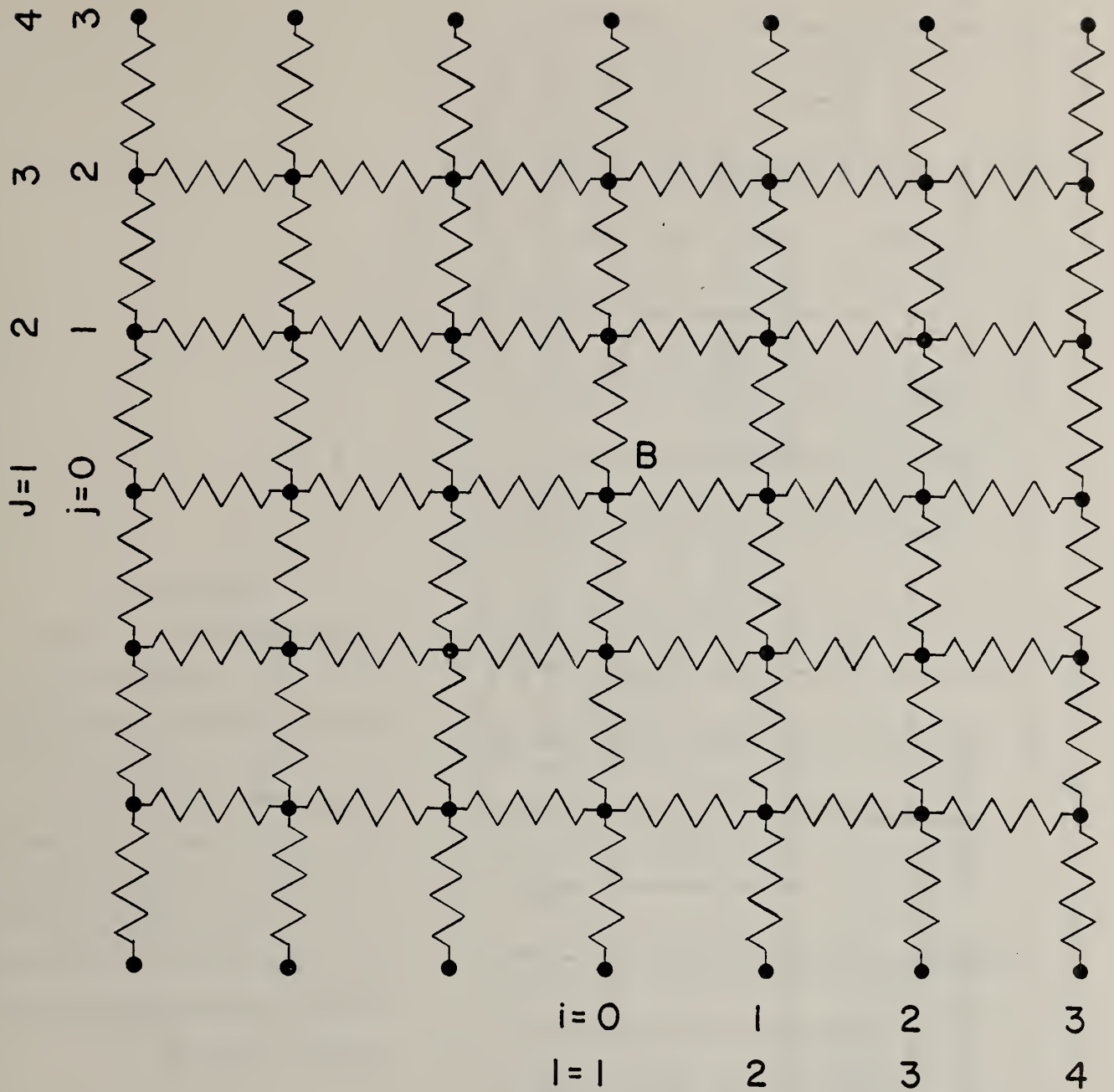
Figure 2.

Schematic representation of square-network model. Model has 2M-1 parallel columns of springs. Each column has 2N-1 junction points which, excepting the end points, are attached to transverse springs.
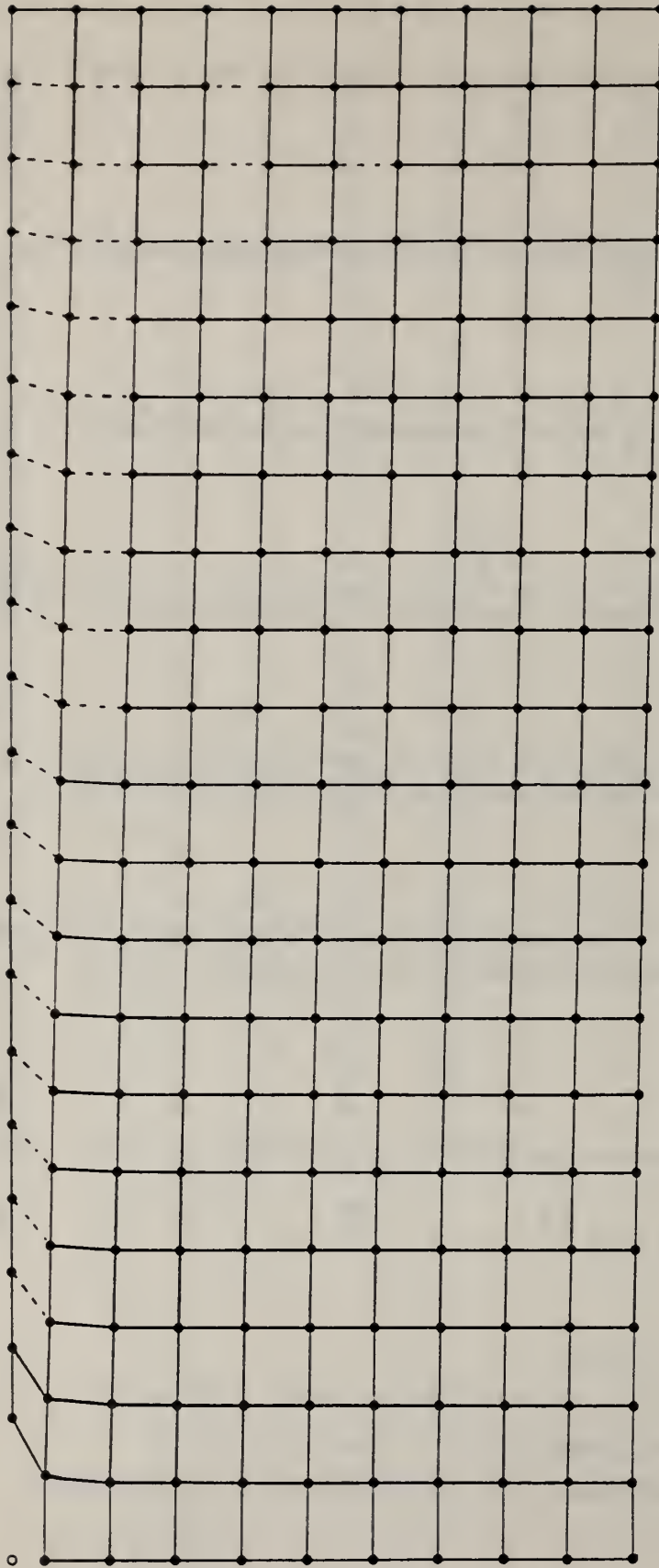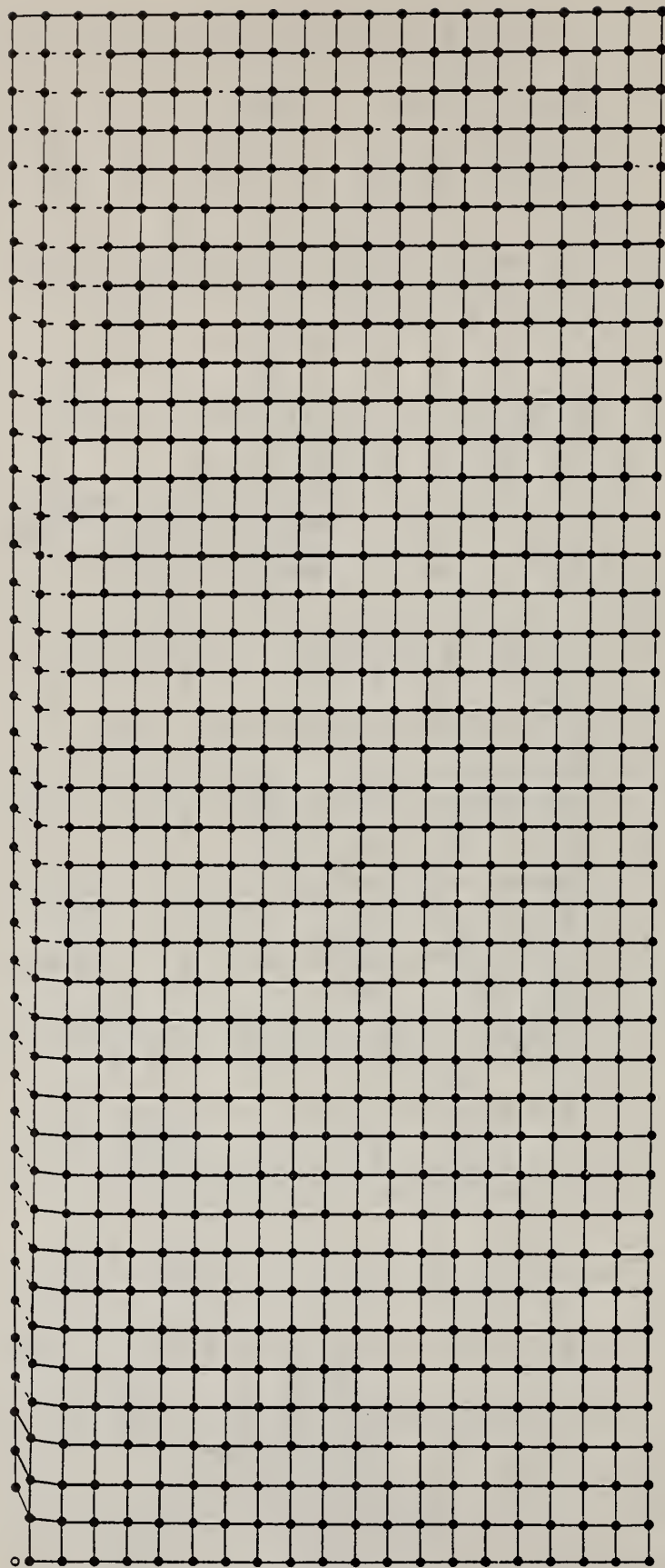
Figure 3.
Configuration of the
positive quadrant of a
square-network model for
which M=11, N=21, after
a central bond break.
The broken bond is desig-
nated by the open circle
in the lower left corner.
Springs in which buckling
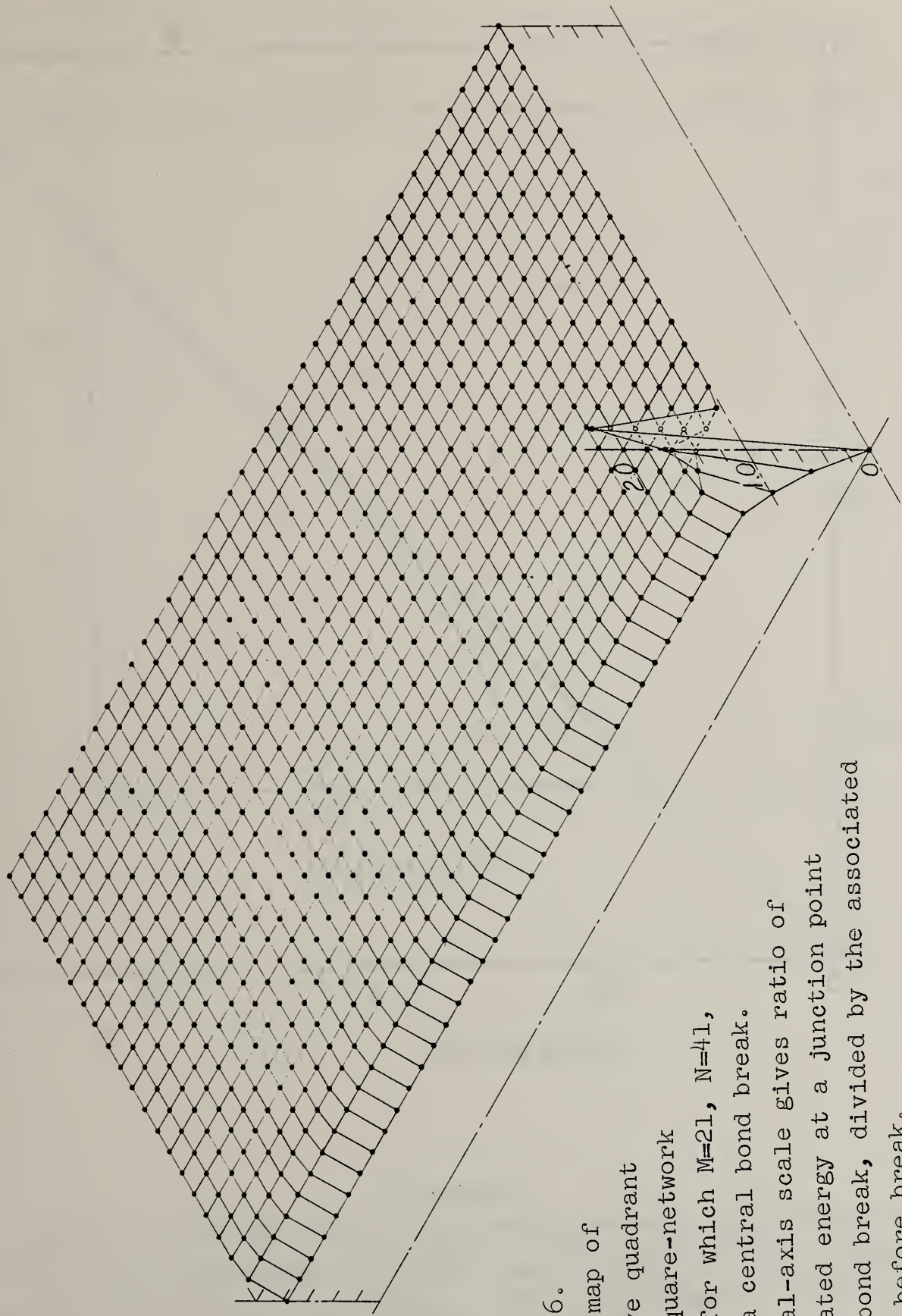occurs are designated by
dashed lines.
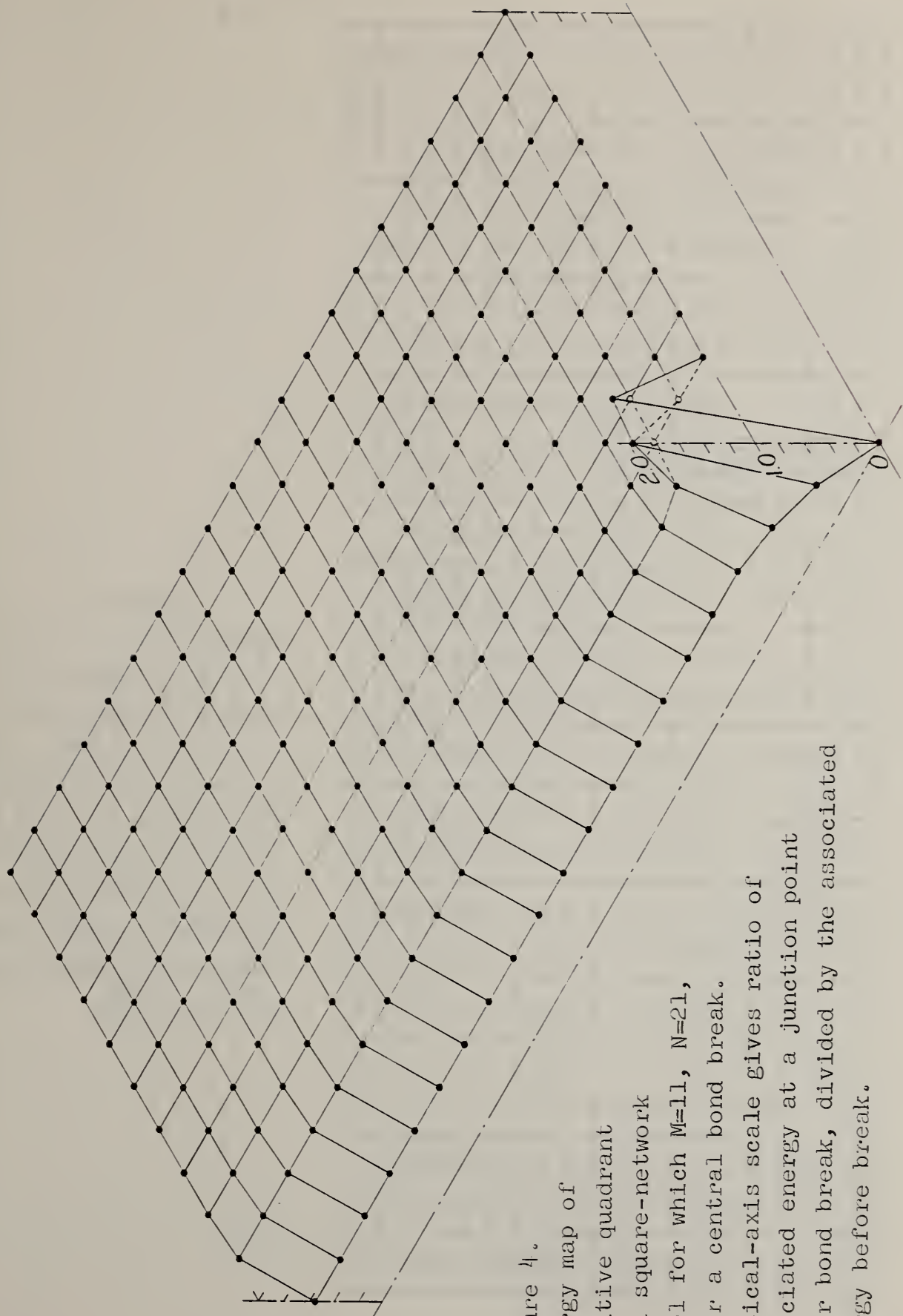
Figure 4.
Energy map of
positive quadrant
of a square-network
model for which M=11, N=21,
after a central bond break.
Vertical-axis scale gives ratio of
associated energy at a junction point
after bond break, divided by the associated
energy before break.

Figure 5.
Configuration of the
positive quadrant of a
square-network model for
which M=21, N=41, after
a central bond break.
The broken bond is desig-
nated by the open circle
in the lower left corner.
Springs in which buckling
occurs are designated by
dashed lines.

Figure 6.
Energy map of
positive quadrant
of a square-network
model for which M=21, N=41,
after a central bond break.
Vertical-axis scale gives ratio of
associated energy at a junction point
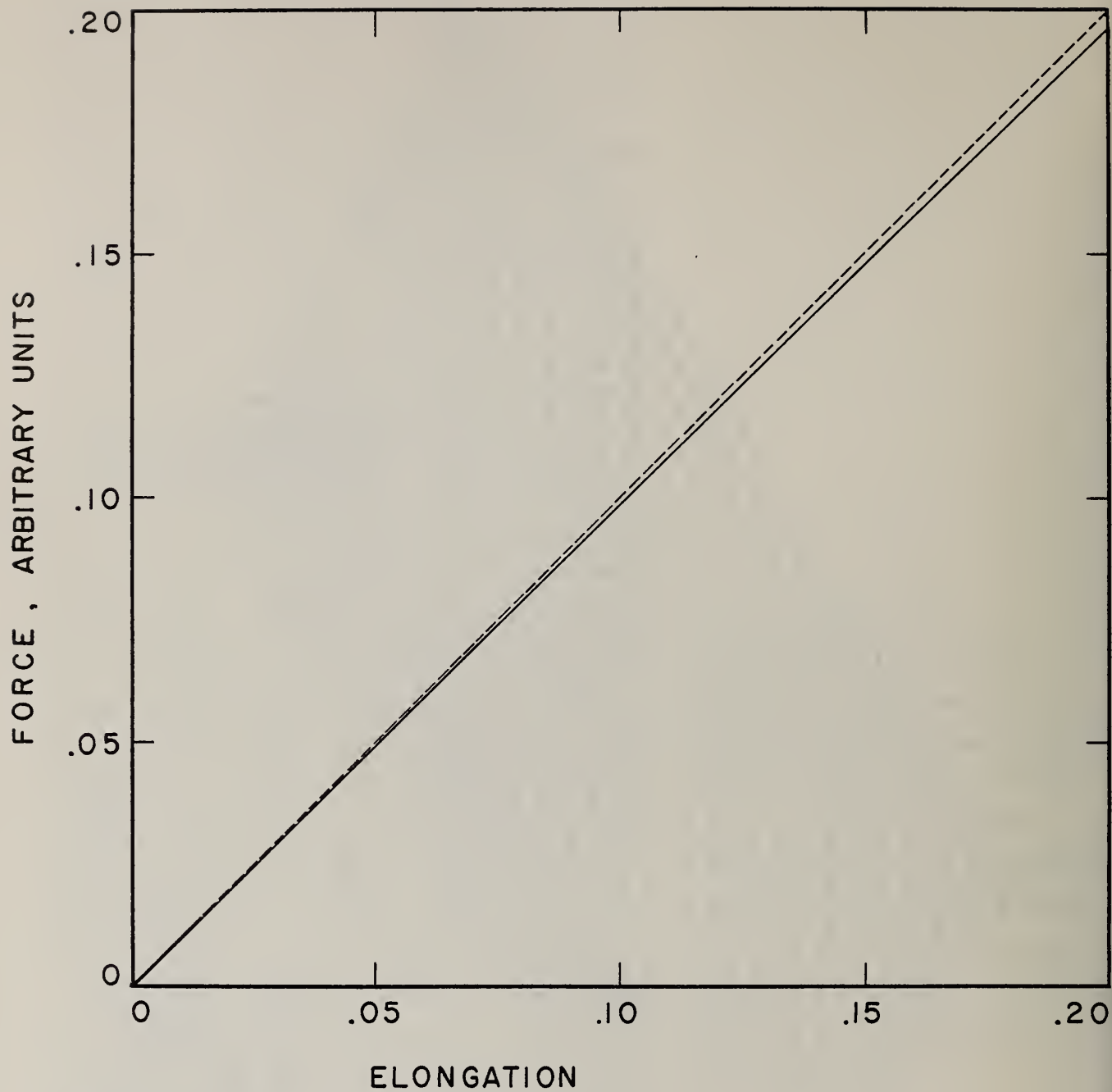after bond break, divided by the associated
energy before break.

Figure 7.

Force-elongation curve after central bond break in a square-
network model for which M=11, N=21. $\overline{T}\delta$ is plotted vs δ, where
δ is the elongation per unit length. Dashed line shows force-
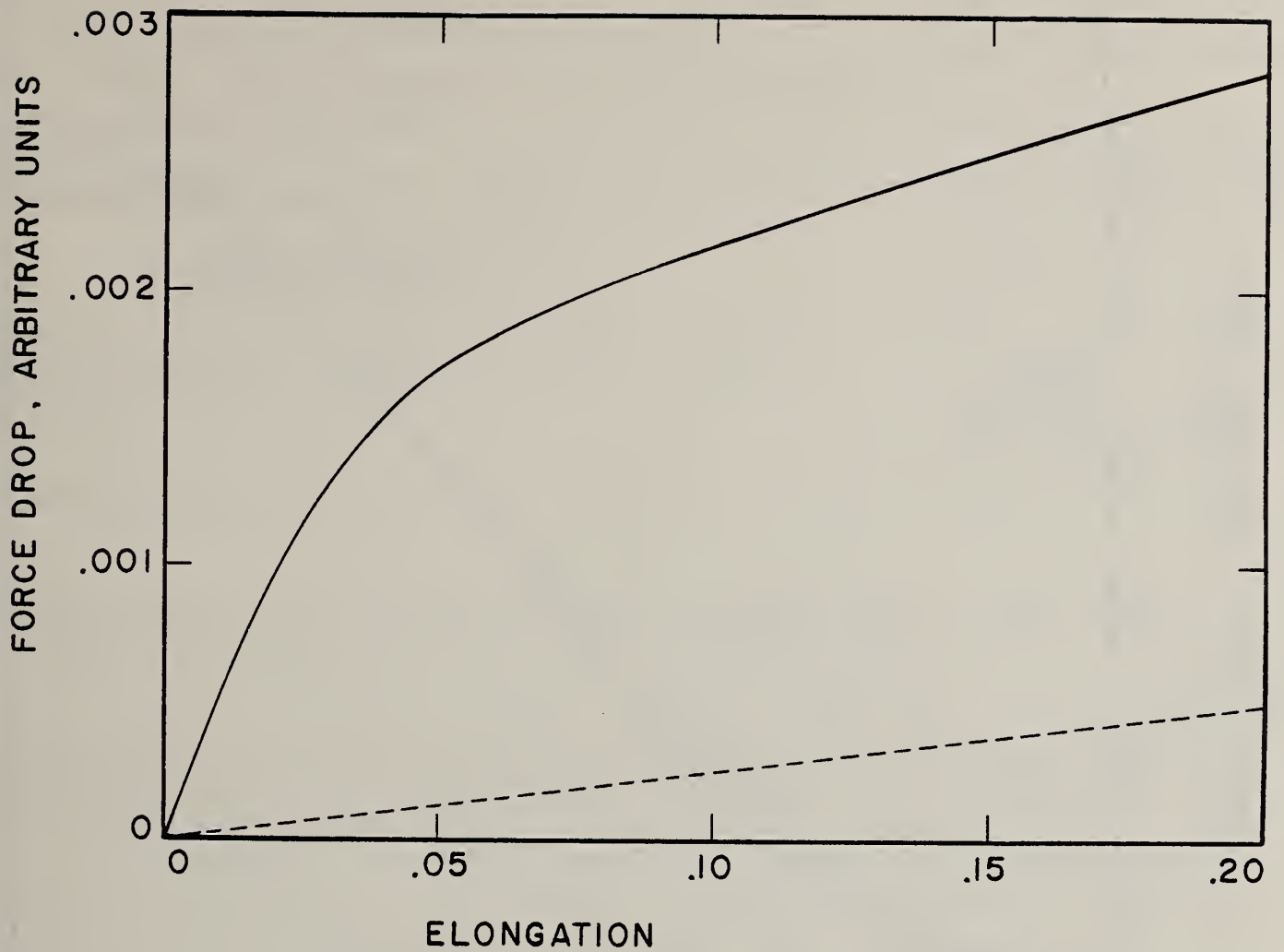elongation curve before bond break.

Figure 8.

Curve of force drop due to bond break vs elongation of a
square-network model for which M=11, N=21. $(1-\overline{T})\delta$ is plotted
vs δ, where δ is the elongation per unit length. Dashed line
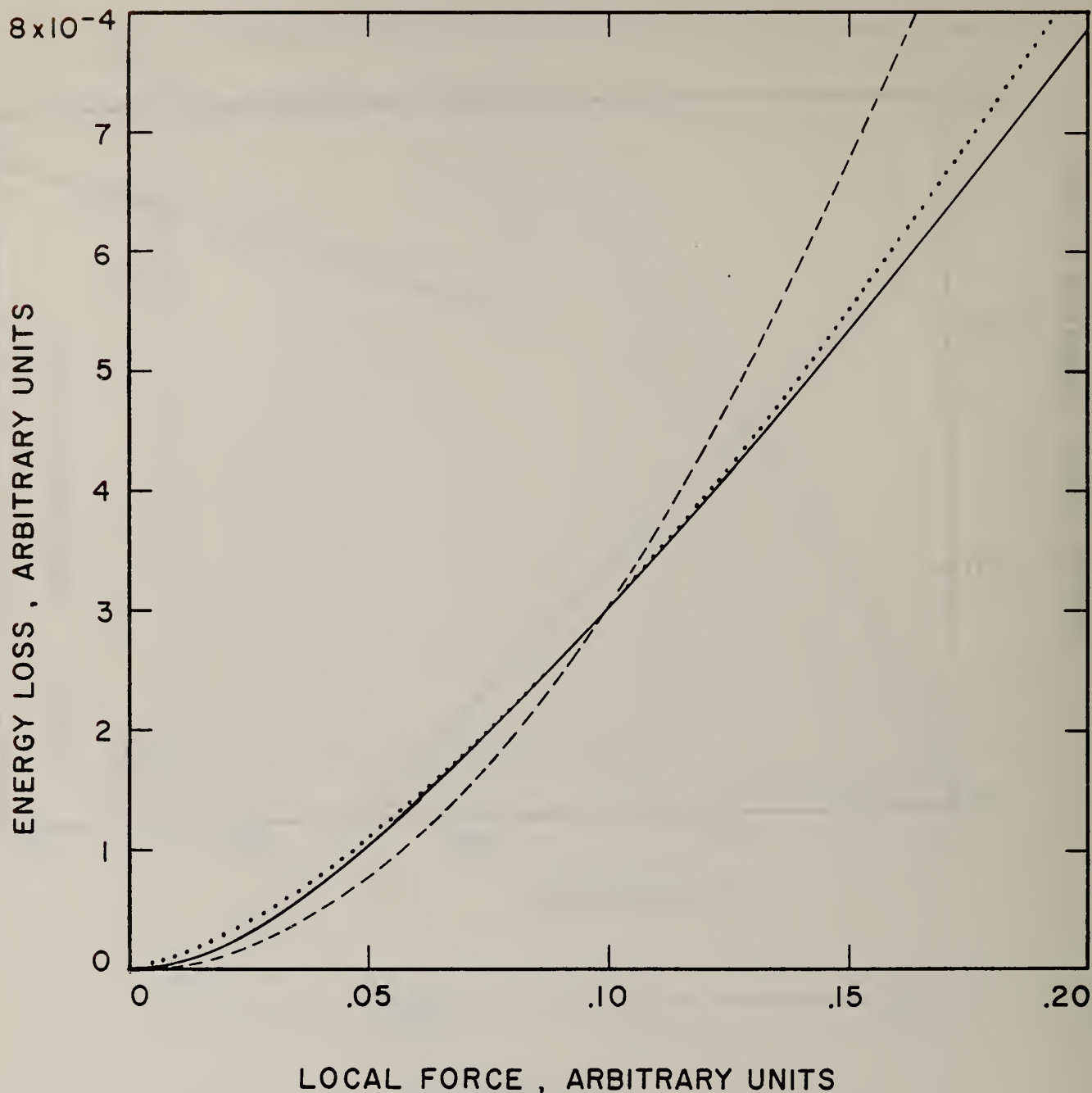shows force drop for equivalent parallel-spring model.

Figure 9.

Curve of energy loss due to bond break vs bond breaking force for a square-network model with M=11, N=21. $(1 - \frac{2N-1}{2N-2}\overline{E})\delta^2$ is plotted vs elongation per unit length δ, which is proportional to bond breaking force. Dashed line is plot of $K\delta^2$ vs δ, and dotted line a plot of $K'\delta^{1.5}$ vs δ. The constants K and K' are adjusted so that ordinates of the plots are equal at δ=0.10 .

U.S. DEPT. OF COMM. BIBLIOGRAPHIC DATA SHEET	1. PUBLICATION OR REPORT NO. NBSIR 79-1735	2. Gov't Accession No.	3. Recipient's Accession No.
4. TITLE AND SUBTITLE Characterizing the Interfiber Bonding of Paper Pulps: Tensile Behavior of Some Mathematical Models of Paper Networks.		5. Publication Date	
		6. Performing Organization Code	
7. AUTHOR(S) Jack C. Smith		8. Performing Organ. Report No.	
9. PERFORMING ORGANIZATION NAME AND ADDRESS NATIONAL BUREAU OF STANDARDS DEPARTMENT OF COMMERCE WASHINGTON, D.C. 20234		10. Project/Task/Work Unit No.	
		11. Contract/Grant No.	
12. Sponsoring Organization Name and Complete Address (Street, City, State, ZIP) U.S. Department of Energy Washington, D. C. 20234		13. Type of Report & Period Covered Final 4/1/77 - 9/30/77	
		14. Sponsoring Agency Code	

15. SUPPLEMENTARY NOTES

16. ABSTRACT (A 200-word or less factual summary of most significant information. If document includes a significant bibliography or literature survey, mention it here.)

The tensile behavior of a thin web-like paper network was simulated by two simple mathematical models. The mesh distortion, drop in tensile force and energy loss resulting from breakage of a network junction were calculated. These results were used to formulate two parameters for characterizing interfiber adhesion: a parameter averaging the network losses incurred in a series of bond breaks when the network is elongated, and a parameter averaging the force drops. The effect of mesh size, local bond adhesive force, and size and shape of the specimen network were calculated. These results based on model studies were used to interpret behavior observed in an actual paper network.

17. KEY WORDS (six to twelve entries; alphabetical order; capitalize only the first letter of the first key word unless a proper name; separated by semicolons)

Mathematical modeling, network; network, tensile properties; paper, interfiber bonding; paper, low-density handsheets; paper, pulp properties.

18. AVAILABILITY ☐ Unlimited		19. SECURITY CLASS (THIS REPORT) UNCLASSIFIED	21. NO. OF PAGES
☒ For Official Distribution. Do Not Release to NTIS			
☐ Order From Sup. of Doc., U.S. Government Printing Office Washington, D.C. 20402, SD Cat. No. C13		20. SECURITY CLASS (THIS PAGE) UNCLASSIFIED	22. Price
☐ Order From National Technical Information Service (NTIS) Springfield, Virginia 22151			